ChemistrySelect
Chemistry Europe
European Chemical Societies Publishing

Impact Factor 2.0
Q3

RESEARCH ARTICLE

Synthesis and Characterization of Copper, Zinc, and Nickel Oxides-Based Nanocomposite by Using *Clitoria ternatea* Flower Extract for Antioxidant Studies and Electrochemical Applications

Sheikdawood Parveen[1] | Kanagaraj Suganthi[2] | Punniyakotti Parthipan[3] | Murugesan Rajasekar[4] | Theivendren Panneerselvam[5] | Arumugam Kosiha[5] | Giriraj Kalaiarasi[2,6]

[1]Bio-Inspired Material Research Laboratory, Dr. Mahalingam College of Engineering and Technology, Coimbatore, Tamil Nadu, India | [2]Department of Chemistry, Karpagam Academy of Higher Education (Deemed to Be University), Coimbatore, Tamil Nadu, India | [3]Department of Biotechnology, Faculty of Science and Humanities, SRM Institute of Science and Technology, Kattankulathur, Chengalpattu, Tamil Nadu, India | [4]Department of Chemistry, K.S.R. College of Engineering, Tiruchengode, Tamil Nadu, India | [5]Department of Chemistry, VELS Institute of Science, Technology & Advanced Studies (Deemed to Be University), Chennai, Tamil Nadu, India | [6]Centre for Material Chemistry, Karpagam Academy of Higher Education (Deemed to Be University), Coimbatore, Tamil Nadu, India

Correspondence: Arumugam Kosiha (kosiha.sbs@velsuniv.ac.in) | Giriraj Kalaiarasi (kalaiarasi.giriraj@kahedu.edu.in)

Received: 3 July 2025 | **Revised:** 10 October 2025 | **Accepted:** 12 November 2025

Keywords: anti-oxidant activity | *C. ternatea* flower extract | copper–zinc–nickel oxides | electrochemical performance | facile green synthesis | nanocomposite (CNZ)

ABSTRACT

The paper presents an eco-friendly method for synthesizing a ternary copper, zinc, and nickel oxides nanocomposite using *Clitoria ternatea* flower extract as the synthesis agent. The bioactive compounds in the extract act as protective agents, facilitating the formation of CNZ and eliminating the need for additional chemical reagents. The synthesized CNZ was characterized using various analytical techniques (UV–Vis, FT-IR, SEM, TEM, PXRD, EDX, and BET), and the obtained results suggest that the formation of the composite (CNZ) and confirm its crystalline nature. TEM image demonstrated that the CNZ has a spherical shape with crystallite size varying between 8 to 20 nm. The optical absorption band gap of the CNZ has been estimated to be 3.37 eV. To explore the application of CNZ in real-world application, we do both biological and electrochemical studies. In biological studies, the anti-oxidant activity of the CNZ has been examined with a series of free radicals, such as DPPH•, $ABTS^{\bullet+}$, $NO^{\bullet}$, and O_2^{-} along with the ascorbic acid (AA) and butylated hydroxy anisole (BHA), and the obtained results showed that the composite possessed substantial activity. For electrochemical applications, we employed cyclic voltammetry (CV), galvanostatic charge–discharge (GCD), and electrochemical impedance spectroscopy (EIS). The CNZ-based electrode exhibited pseudocapacitive behavior, with a specific capacitance of 387.7 F g^{-1} at 1 A g^{-1}, demonstrating improved charge storage. The electrode retains 90% of its specific capacitance from the initial value after repeated charge–discharge processes for 2000 cycles. Ultimately, the combined electrochemical and antioxidant performance makes CNZ nanoparticles derived from *C. ternatea* flower extract a promising subject for further research.

1 | Introduction

Nanoparticles alongside multifunctional nanomaterials have received notable interest because they provide solutions to numerous application fields, including catalysis and wastewater treatment as well as bioimaging and cancer therapy [1]. Due to better performance and higher selectivity properties, trimetallic nanoparticles surpass both monometallic and bimetallic nanoparticles in potential applications. Synthesis of nanomaterials through different approaches, including physical, chemical, and biological methods, takes place because of their widespread applications [2–5]. Plant-assisted synthesis of nanomaterials stands out as an optimal method because of its eco-friendly benefits, although chemical and physical techniques encounter limitations that include toxicity risk and high energy expenses. Mixed metal oxide systems are distinctive structures that integrate various characteristics of metal oxides. Due to these properties, they play a vital role in energy storage applications [6].

The highly unstable free radical molecules derived from different chemical mechanisms create molecular instability by stealing electrons from molecules, thus inflicting molecular damage. Foreign substances produced by reactive species cause damage to DNA and proteins together with lipids, resulting in major medical conditions such as cancer, neurological issues, and heart disease. Nanomedicine through radical scavenging appears to present a viable solution for minimizing such harmful biological outcomes because the situation requires immediate effective intervention [7–9]. Researchers focus strongly on nanomaterials because of their special physicochemical characteristics. The commercial demand for nanomaterials triggered the production of numerous products across various application fields. Multi-metallic NPs demonstrate various electronic and optical and magnetic behaviors whose properties stem from size, along with the shape of the nanomaterials and the potential on their surface characteristics [10, 11]. The properties of nanomaterials allow their efficient contact with bacterial membranes, which produces disruption and reactive oxygen species formation and leads to protein destruction, DNA damage alongside bacterial cell death together with host immune system activation [12, 13]. The production of nanoparticles through plant extracts together with microorganisms or chemical/physical methods as a fundamental production method. Phyto compounds/plant-mediated nanotechnology represents a new sustainable production method which utilizes plant leaves and other organic components together with seeds, roots, and fruits to synthesize nanoparticles at affordable costs. Active plant materials and their bioactive metabolites consisting of polysaccharides and terpenoids alongside alkaloids, as well as organic acids and proteins and vitamins, participate in these synthetic routes [14].

The extensive scientific investigation has focused on understanding the biological attributes of metal oxide nanoparticles specifically CuO, ZnO, and NiO. The evaluated copper-based devices were used to determine their antimicrobial effects on *Escherichia coli*, *Vibrio cholerae*, and *Salmonella typhi* bacteria, whereas researchers examined the cytotoxic properties and antioxidant characteristics of ZnO particles extracted from *Mangifera indica* leaves when using high-concentration solutions [15, 16]. The sol–gel method enables scientists to produce pure nanoparticles of ZnO, CuO, and Fe_2O_3 metal oxides [17]. The antibacterial potency of these nanoparticles shows that their antibacterial properties directly correspond to their surface-to-volume ratio, where ZnO nanoparticles display the strongest antimicrobial effectiveness.

Plant extracts play a vital role in preparing a metal oxide and mixed metal oxides nanoparticles. The authors synthesized CuO/ZnO/NiO nanocomposites using *C. ternatea* flower extracts, which were obtained from fresh plants belonging to the Fabaceae family. *C. ternatea* flowers possess numerous pharmacological properties due to the phytochemical compounds in which it contains tannins, triterpenoids, phenols, alkaloids, flavonoids, anthraquinones, glycosides, proteins, volatile oils, and steroids [18]. Throughout history, people have used different plant components from *C. ternatea* to cure stomach pain, skin diseases, sore throats, and improve mental capabilities. The aerial parts of *C. ternatea* flowers serve together with other plant parts as snakebite antidotes [19].

The extract of *C. ternatea* serves as a bridge between the phytochemistry, nanotechnology, and sustainability. There were several reports that depict the use of the extract of *C. ternatea* flower to synthesize metal oxide nanoparticles. Sharma et al. synthesized SrO_2 NPs with the assistance of *C. ternatea* flower extract and studied their biological applications [20]. Similarly, Guttapalli et al. used *C. ternatea* extract to synthesize the ZnO–rGO NP and reported their biological applications [21]. Kachhawaha et al. presented the FeO NP by *C. ternatea* extract and reported their anti-microbial applications in *E. coli* [22]. Prabhu et al. synthesized metal oxides of Cu, Ni, and Zn separately and studied their photocatalytic dye degradation in dyes along with that their anti-microbial nature in gram-negative *E. coli* and *S. aureus*, and obtained promising results in the research [23–25]. Alahmdi et al. presented ZnO NP by *C. ternatea* flower extract and reported its anti-cancer application in MCF-7 cell line [26]. Chan et al. synthesized the Fe and Ag-doped ZnO nanoparticles by *C. ternatea* extract and used this to enhance the sonocatalytic degradation of Congo red dye [27]. Satpathy et al. synthesized Cobalt oxide nanoparticles from the *C. ternatea* flower extract and presented their neuroprotective actions at low doses [28]. Lavanya et al. reported the synthesis of MgO NP from *C. ternatea* extract and studied their impact on plant growth, soil dynamics, and computational analysis [29].

The extract of *C. ternatea* possesses high levels of anthocyanins, flavonoids, polyphenols, alkaloids and etc., which shows improved dispersion and reduced agglomeration mechanically. The molecules, such as anthocyanins, act as both reducing and stabilizing agents. In our synthetic procedure, we prepare the nanocomposite (**CNZ**) in a single step at room temperature. This process produces a stable CuO/ZnO/NiO nanocomposite with a uniform size and good electrochemical activity. Further, the nanocomposites formed by these constituents showed potent biological activities. This method has a significant improvement compared to an older green synthesis method, which often creates uneven particles and needs some extra steps to stabilize them.

According to the aforementioned facts, the study investigates an original method to synthesize CuO/ZnO/NiO nanocomposite through *C. ternatea* flower extract, which has not been studied previously [20–29]. The research conducts a complete antioxidant evaluation of the synthesized nanocomposite, which

stands as the initial research into ZnO/CuO/NiO ternary metal oxide nanocomposites prepared from *C. ternatea* flowers. The nanocomposite synthesized by the extract of *C. ternatea* show good anti-oxidant activity with a series of radicals than some other nanocomposites from other plant extracts [30]. This research analyzes how the synthesized nanocomposites improve biological functions while producing significant findings applicable to creating medical nanomaterials that fight against stress-altered diseases. In addition to the biological evaluation, we examine the electrochemical behavior of the synthesized tertiary metal oxides nanocomposite.

2 | Experimental Work

2.1 | Plant Identification and Its Phytochemistry

C. ternatea belongs to the family Fabaceae. The height of a *C. ternatea* plant can range from 30 to 450 cm. The flower contains phenolics, flavonols like ternatins, quercetin, myricetin, and kaempferol derivatives. The seeds contain palmitic, stearic, oleic, linoleic, and lonolenic acids. Complex chemical components found in leaves and fruits produce alkaloids and various kinds of proteins with greater economic significance. Formation of nanocomposites by using plant extract follows a mechanistic pathway of reduction of metal ions, nucleation growth, stabilization, and capping.

C. ternatea comprises diversified phytochemicals, as mentioned above; each phytochemical has its distinctive role in the nanoparticle formation, like flavanols and fatty acids act as the reducing agents by reducing the oxidation state of metal ions and stabilization. Flavonols have many hydroxyl groups that give electrons to metal ions, turning them into nanoparticles. They also stick to the surface of the nanoparticles to keep them stable. Fatty acids have carboxyl groups that attach to the nanoparticles and help to keep them stable. These compounds allow the formation of nanoparticles easily at normal conditions. The fatty acids, oleic acid-mild reducer, prevent agglomeration by forming hydrophobic layers and act as a dispersion aid, linoleic acid-surface stabilization via unsaturated bonds, palmitic acid-hydrophobic capping, stearic acid-stabilization, emulsification, and particle size controller [31, 32]. Phenolic compounds lend the electron-donating groups (reduction, capping, and improve dispersion), alkaloids aids in nucleation growth control, saponins and tannins act as the emulsifiers, stabilizers, surface functionalization, and colloidal stability [21, 22]. Recent studies show that the type and amount of these chemicals present in the plant extract affect the size, shape, and stability of the nanocomposites. This affects how they are used in catalysis, medicine, and cleaning the environment. *C. ternatea* has a wide variety of medical applications, such as in traditional ayurvedic medicine has been used for centuries as a memory enhancer, nootropic, antistress, anxiolytic, antidepressant, anticonvulsant, and sedative agent [33, 34].

2.2 | Preparation of Plant Extract

The authors collected the plant specimen *C. ternatea* flowers from the Eachanari region in Coimbatore. The collected *C. ternatea* flowers were washed several times with tap water and then with distilled water to remove the impurities and dried in sunlight for 4 days. Initially, 10 g of sundried *C. ternatea* flowers were weighed and charged into the 250 mL conical flask. To this flowers 100 mL of de-ionized water (freshly prepared) was added as the medium of extraction. Then the conical flask was placed in a temperature-controlled water bath to ensure the consistent performance, and the temperature was set to 80°C, and it was heated up to 4 h for the extraction of phytochemicals from the flowers. Due to the undisturbed continued heating, color of the water changed from colorless to dark blue. After, the extract was allowed to cool at room temperature. Once cooled, the extract was filtered through Whatman no. 1 filter paper to remove the flower residues from the aqueous extract. The resultant liquid contains the phytochemicals from *C. ternatea* flower, which can be used to synthesize nanocomposites [35].

2.3 | Facile Synthesis of Nanocomposite-Copper, Zinc, and Nickel Oxides Composite (CNZ)

The researchers prepared each 100 mM solutions of $Cu(NO_3)_2.3H_2O$ (0.003 mol; 0.725 g in 30 mL of *C. ternatea* flower extract), $Zn(NO_3)_2.6H_2O$ (0.003 mol; 0.892 g in 30 mL of *C. ternatea* flower extract) and $Ni(NO_3)_2.6H_2O$ (0.003 mol; 0.872 g in 30 mL of *C. ternatea* flower extract). For the synthesis of CNZ, all three metal nitrate solutions were taken in equimolar ratio as 1:1:1. In the synthesis procedure, each metal solution was combined together and thoroughly mixed with a magnetic stirrer. A few drops of 0.2 M NaOH solution were added to the mixture, and the stirring was maintained for about 10 h at room temperature. The obtained precipitate was filtered and it underwent evaporation until it became powder. Further, it was calcinated in a muffle furnace at 600°C for 4 h to obtain copper, zinc, and nickel oxides composites (CNZ). During the precipitation process, the pH level was controlled by the 0.2 M NaOH solution, and it stayed around 10.5. This pH level is important for controlling the size and shape of the metal oxide particles. At this alkaline pH, metal ions react with water and form their hydroxides that settle out easily. These hydroxide precursors then change into oxide nanoparticles when heated. These elevated amounts of OH^- ions support the nucleation growth further and leading to a smaller size particle, good crystallinity, quicker hydrolysis of metal precursors [36–38]. The CNZ nanocomposites were calcinated at 600°C. This temperature improves their crystallinity, surface area, and functional properties, without causing the particles to clump together or grow too large, and shows a maximum band gap, which is good for electrochemical applications. Even though high temperature increases the crystallinity but this 600°C provides a good balance between making the particles crystalline enough and keeping them small, which is important for various applications and environmental uses [39]. Multiple analytical methods were used to analyze the structure of CNZ. The supporting information comprised a complete description of instrumentation methods.

2.4 | Electrochemical Performances

The electrochemical testing of synthesized nanocomposite material was conducted through cyclic voltammetry (CV), galvanostatic charge–discharge (GCD), and electrochemical impedance

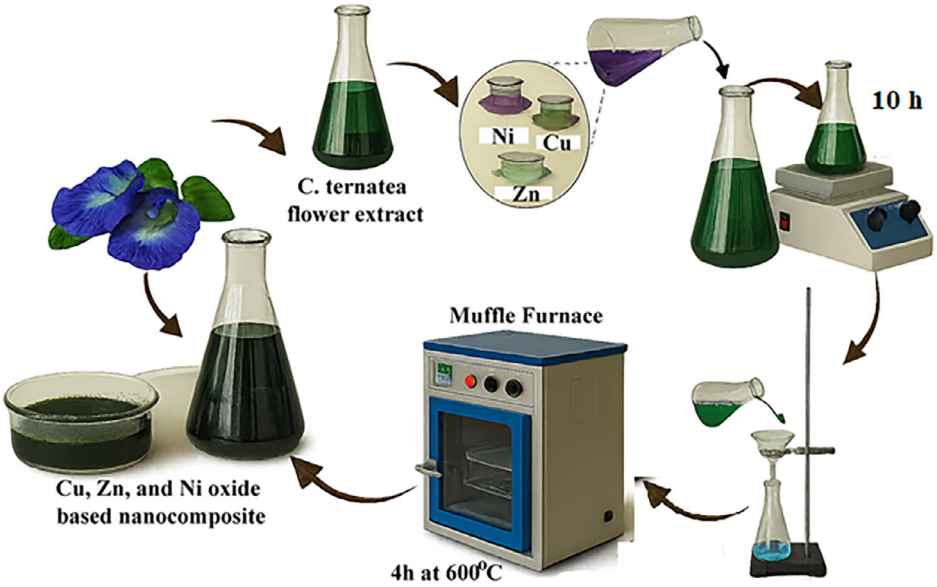

SCHEME 1 | Synthesis process of Cu, Zn, and Ni oxides appended nanocomposite (**CNZ**) using aqueous extract of *C. ternatea* flowers.

spectroscopy (EIS) methods according to the previously reported method [40].

2.5 | Antioxidant Activity

The anti-oxidant activity of the synthesized CNZ and the standards (AA and BHA) has been examined according to the reported methods with a range of free radicals, including $ABTS^{\bullet+}$, $DPPH^{\bullet}$, O^{2-}, and $NO^{\bullet}$ at varying concentrations (20–100 $\mu g mL^{-1}$) [41–44]. Assuring consistency, all experimental measurements were carried out in triplicate ($n = 3$). Three independent replicates are used to calculate the mean ± standard deviation (SD), which is how quantitative data are reported. The standard deviation was selected to represent measurement variability. In all the figures, error bars are included, which show standard deviations. In a plot, if the error bars are not visible, it means that they are inside the bounds of the symbol [45].

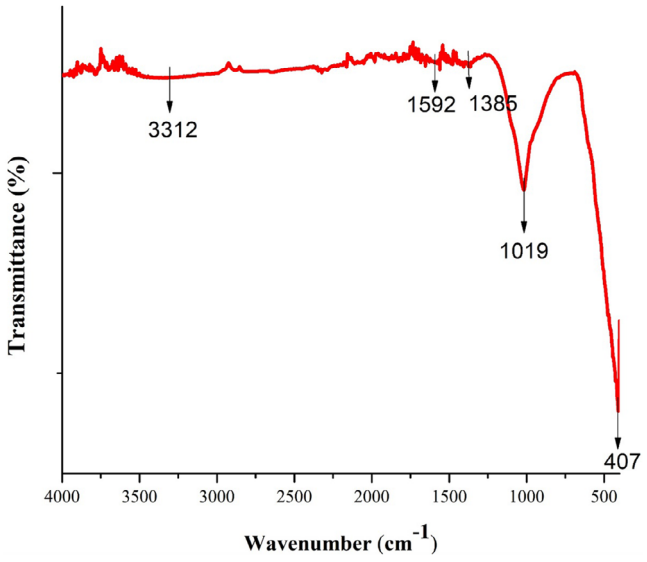

FIGURE 1 | FTIR spectrum of CNZ.

3 | Results and Discussion

Our main aim was to prepare tertiary metal oxides (copper–zinc–nickel) based nanocomposite (**CNZ**) with the help of plant-based compounds without wasting any chemical resources. Corresponding metal nitrates were dissolved with aqueous flower extracts of *C. ternatea* for the production of mixed metal oxides. An aqueous flower extract of *C. ternatea* encompasses alkaloids, flavonoids, saponins, tannins, and glycosides, which may be helpful in reducing metal nitrates to metal oxides appended nanocomposite. The synthetic route of the **CNZ** was given in the Scheme 1.

3.1 | FT-IR Spectroscopy

Figure 1 shows the FT-IR spectrum of the **CNZ** that presents the bending vibration of —OH appear as the sharp band at 1019 cm^{-1} due to the surface hydroxyl group [46, 47]. Additionally, the M—O bond stretches from 800 to 400 cm^{-1} and provides evidence for the CuO/NiO/ZnO nanocomposite. The band at 407 cm^{-1} corresponds to M—O stretching and bending vibrations of the nanocomposite structure [48]. The broad band observed at 3312 cm^{-1} is related to stretching vibrations of O—H, which often caused by moisture or residual hydroxyl groups. This FTIR spectrum also shows some small peaks in the range of 1300–1600 cm^{-1} related to organic residues from plants, such as C—H, C═O, C═C, N—H, and aromatic ring vibrations. The diminishing of the IR bands of the plant residue was due to the calcination process at higher temperatures [49, 50]. The IR spectrum of CNZ was compared with the pure metal oxides like CuO, ZnO, and NiO, which were synthesized chemically without any green extract [51–56]. The peaks corresponded to the organic residues were not present in pure metal oxides made without

plant extracts. The observed results indicated that the presence of organic molecules in the CNZ act as the capping and stabilizing agents.

3.2 | UV–Visible Spectroscopy

In solid form, the generated composite's UV spectrum was captured (Figure S1). Similar to previous observations, the CNZ produced from *C. ternatea* flower extract exhibited maximum optical absorption bands at 367 nm as a result of the metal cation d-d transitions. Additionally, using the Equation (1).

$$Eg = 1240/\lambda \tag{1}$$

The band gap energy (*Eg*) was determined to be 3.37 eV [48, 57]. The band gaps of the individual metal oxides usually range from 1.2 eV, 3.6–4.0 eV, and ~3.3 eV for CuO, NiO, and ZnO, respectively. The obtained band gap for CNZ was 3.37 eV, and this was neither as small as copper nor greater as NiO. The optical properties of the ternary CNZ were different from the individual metal oxides due to the different molar ratio of metals in it and the synthetic conditions [58, 59].

These difference in band gaps of the individual metal oxide counterparts creates type-II heterojunctions in CNZ nanocomposite, which facilitates directional electron flow, reduced recombination rates and efficient charge separation and modifies the DoS (Density of States) and enhances carrier mobility. Doping of metal ions creates defects and provides mid-gap energy levels which have good visible-light absorption, improved redox activity and conductivity, and narrows the effective band gap [60, 61].

3.3 | X-Ray Diffraction (XRD) Analysis

The powder XRD analysis determined both crystallite structure and crystallite size measurement for the synthesized nanocomposite. The powder XRD pattern of the synthesized CuO/NiO/ZnO nanocomposite appears in Figure 2. As a result of X-ray diffraction analysis, we obtained nanocomposite patterns showing well-defined and strong peaks that demonstrate high crystallinity of the synthesized **CNZ**. The (111) and (200) peaks verify the cubic structure of the produced nickel oxide nanoparticles according to JCPDS: 47–1049 [62]. Measurement points at 2θ = 37.2, 63.5, and 68.1° demonstrate the hexagonal primitive phase of ZnO nanocrystals that corroborate with JCPDS: 79–2205 [63]. The nanocomposite contains monoclinic CuO nanoparticles whose short peak positions at 2θ = 33.23, 48.9, and 56.8 degrees match the (111), (202), and (021) hkl plane values listed in JCPDS: 05–0661 [64]. The peaks appearing at 2θ = 75.1 and 58.2° with hkl values of (311) and (220) indicated cubic phase CuO–NiO (JCPDS: 78–0648) and NiO–ZnO (JCPDS: 75–0270) [65]. The Debye Scherer formula Equation (2) allowed determination of the average crystallite size for the synthesized CuO/ZnO/NiO nanocomposite.

$$D = 0.9\lambda/\beta cos\theta \tag{2}$$

The calculation depends on λ representing X-ray wavelength together with β representing full width at half maximum peak

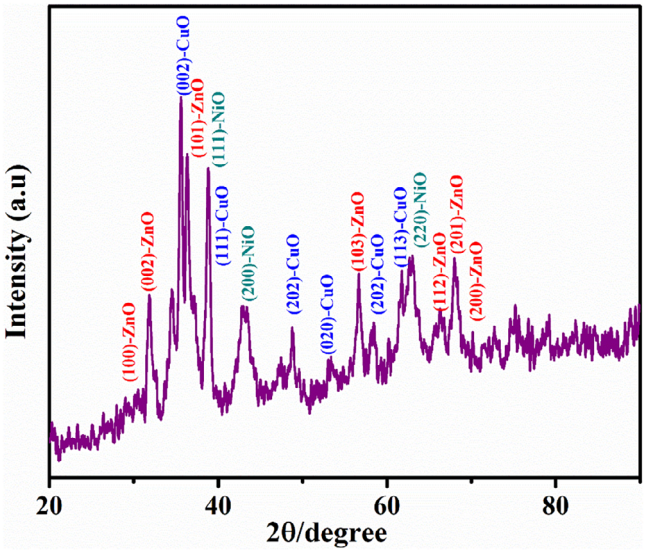

FIGURE 2 | PXRD patterns of CNZ.

values while the Scherer constant equals 0.9 [66]. The X-ray analysis revealed that synthesized nanocomposite show an average crystallite size measure at 29 nm through the application of the Scherer formula.

Additionally, the crystallite size of synthesized material was ascertained using the Williamson–Hall plot [67]. The Williamson–Hall (W–H) equation for XRD analysis is Equation (3):

$$\beta \cos\theta = \frac{K\lambda}{\mathrm{D}} + 4\varepsilon \sin\theta \tag{3}$$

In the Equation (3), β is the observed peak width (full width at half maximum), the dimensionless shape factor (about 0.9), X-ray wavelength (0.154 nm for Cu), and crystallite size are the parameters of K, λ, and D, respectively. The resulting crystallite size is 24.13 nm [68]. The obtained slope (Figure S2) indicates that the crystallite size as calculated by the Williamson–Hall plots is smaller than the Scherer equation because of non-zero residual tension. Furthermore, it was noted that the material had a micro strain value of roughly 0.178×10^{-3}.

3.4 | Scanning Electron Microscopy

The SEM image of the synthesized nanocomposite (**CNZ**) appears in Figure 3. The SEM image revealed that the background contained dense agglomeration together with empty spaces at specific locations. The complex structure showed visible boundaries on its surface, together with one or more individual particles. The individual particles within the complex showed non-uniform forms in addition to their irregular shapes [69].

3.5 | Surface Characterization (BET Analysis)

BET analysis is used for composites to determine their specific surface area and pore characteristics, which are crucial for applications like catalysis, energy storage, and drug delivery. The surface properties, such as surface area and the influence of

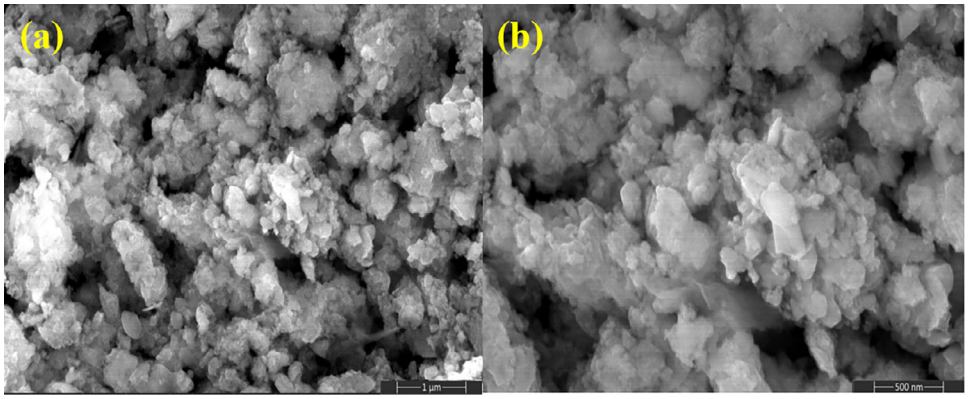

FIGURE 3 | FE-SEM micrographs (a) SEM images of CNZ at 1 µM (b) SEM images of CNZ at 500 nm.

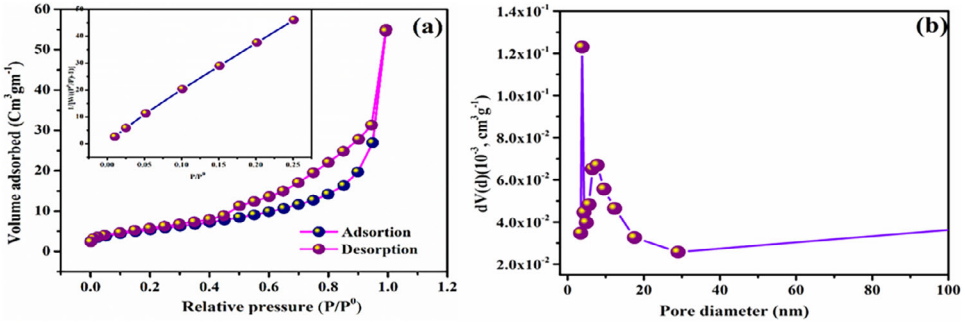

FIGURE 4 | (a) N2 adsorption–desorption isotherm; (b) pore size distribution of the composite.

synthesis process on porosity, were further investigated using Barrett–Joyner–Halenda (BJH) pore size distribution analysis, nitrogen adsorption–desorption measurements, and Brunauer–Emmett–Teller (BET) analysis. The amount of gas adsorbed at various pressures is measured, and the data is analyzed using the BET equation to calculate the total surface area, pore volume, and pore size distribution [38, 70]. Figure 4a depicts the sample's N_2 adsorption–desorption isotherms. It exhibits a type IV isotherm with an H_2 hysteresis loop in the relative pressure range of 0.4–1.0 P/P0, the presence of mesopores and macropores possibly formed by the loose stacking of constituent nanoparticles [71].

A homogenous particle size distribution with constant mesoporous channels could be predicted by the average pore sizes, which range from 2 to 25 nm (Figure 4b). It is noteworthy for having the largest BET surface area, measuring 18.98 m^2g^{-1}. Improved capacitive performance is correlated with this larger surface area. It seems that the produced composites' structural integrity influences their porosity and, in turn, their electrochemical performance.

3.6 | Transmission Electron Microscopy

TEM is a microscopy technique used to determine the size of nanoparticles. Figure 5 displays the TEM image **CNZ** captured in bright field mode. The analysis of the TEM image revealed that the particles exhibited a spherical shape and were in a non-agglomerated state. Additionally, the size of the colloidal CNZ nanocomposites varied between 8 and 20 nm. The average crystallite size obtained from XRD may not be equal to the particle size obtained from TEM as a single particle can consist of more than one crystallite, further possibly due to particle agglomeration, polydispersity, or differences between grain size and crystallite size [50]. Further, selected area electron diffraction (SAED) patterns (Figure 5f) from a selected area of the TEM images exhibited notable ring-like patterns, which indicate their polycrystalline nature.

3.7 | Energy-Dispersive X-Ray Spectroscopy (EDAX)

The elemental composition of the prepared **CNZ** was examined by the EDAX technique. Depending on weight and atomic fraction, EDAX spectra energies vary from 0 to 10 keV. Zinc, nickel, copper, and oxygen peaks were well-built in the sample's spectrum (Figure 6). Presence of metals composition in the composite was given in Table 1, indicated that Zn (22.77), Ni (16.73), Cu (38.45), and oxygen (22.25) with percentages, respectively. Nanoparticle composition was indicated by EDAX spectra, the obtained composition data matched theoretical values.

3.8 | Electrochemical Performances

Tests of the electrochemical performances for synthesized nanocomposite materials included CV alongside GCD, and EIS.

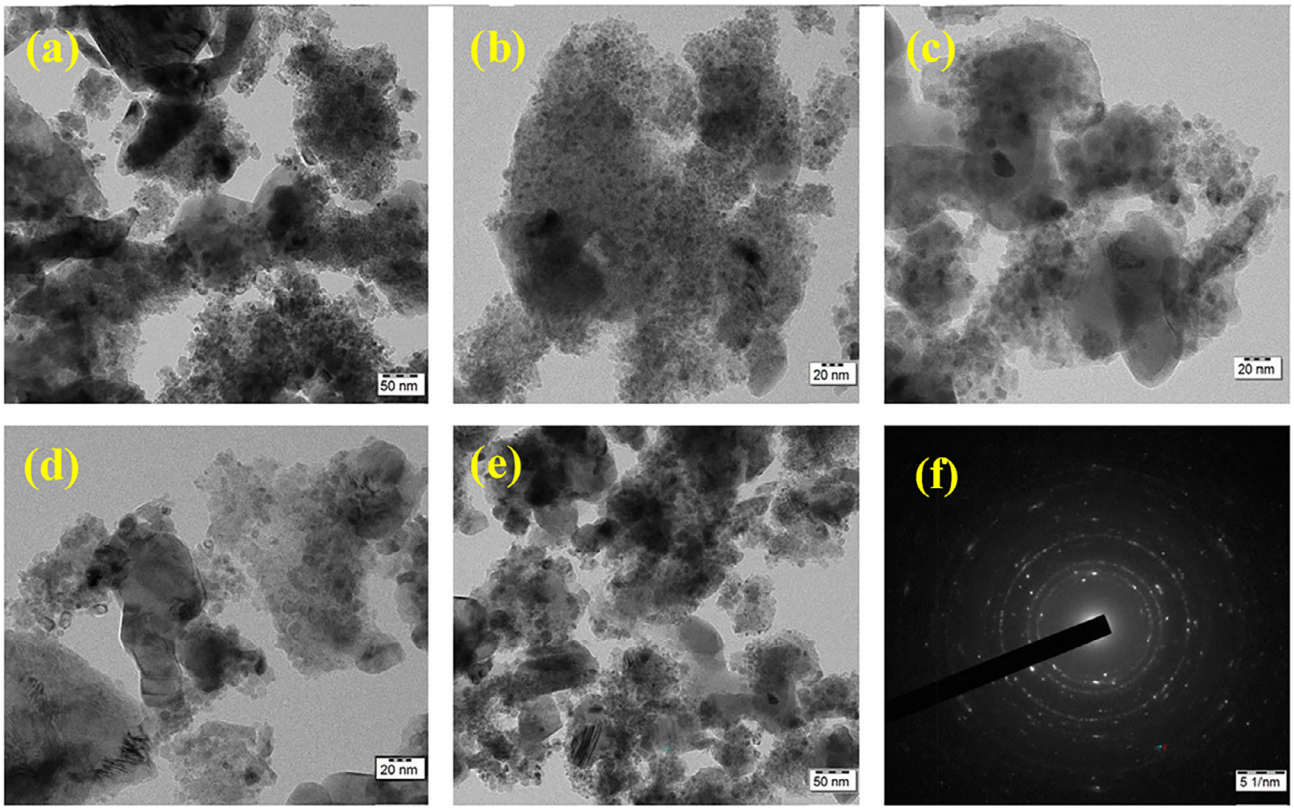

FIGURE 5 | (a–e) TEM micrographs of CNZ at 50 and 20 nm; (f) selected area electron diffraction (SAED) pattern of CNZ.

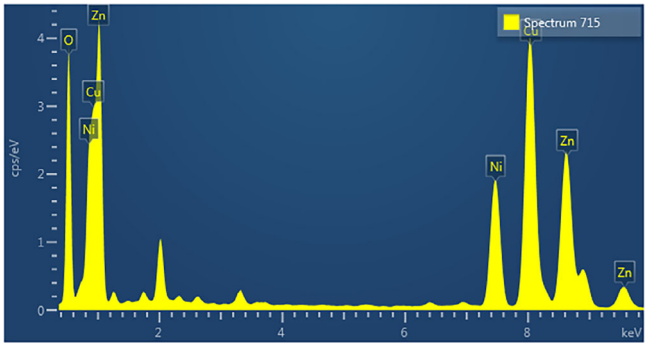

FIGURE 6 | EDAX spectrum of CNZ.

CV studies utilized nanocomposite CNZ as the working electrode together with platinum and calomel electrodes serving as counter electrode and reference electrode during analysis in 6 M aq. KOH electrolytes through a 3-electrode system. CV results in Figure 7a demonstrate **CNZ** behavior across 0 to 0.5 V potential range at a scan rate of 100–5 mVs^{-1} thereby showing non-rectangular pseudocapacitive formation as the intercalation produces these shapes [72]. Good electrochemical stability alongside full reversibility of the electrodes can be attributed to constant CV curve shapes when performing various scan rates. This finding supports an intercalation/surface diffusion-controlled mechanism in redox processes [73].

The charge–discharge tests were carried out with current densities from 20 to 1 Ag^{-1} are shown in Figure 7b. The electrodes displayed non-linear curves in the test, which confirmed their pseudocapacitive behavior while matching the CV profile results. The specific capacitance evaluation resulted in 387.7 Fg^{-1} values for CNZ electrodes at 1 Ag^{-1}. The discharge time of the CNZ electrode demonstrates improvement when using an applied current of 1 Ag^{-1}. The electrochemical performance of CNZ improves due to two factors: its expansive surface area and the increased participation of ions for conductivity. The utiliza-

TABLE 1 | The elemental composition of the CNZ.

Element	Line type	k factor	Absorption correction	Wt%	Wt% sigma	atomic %
O	K series	2.020	1.00	22.05	0.42	52.67
Ni	K series	1.164	1.00	16.73	0.31	10.89
Cu	K series	1.247	1.00	38.45	0.43	23.13
Zn	K series	1.277	1.00	22.77	0.39	13.31
Total:				100.00		100.00

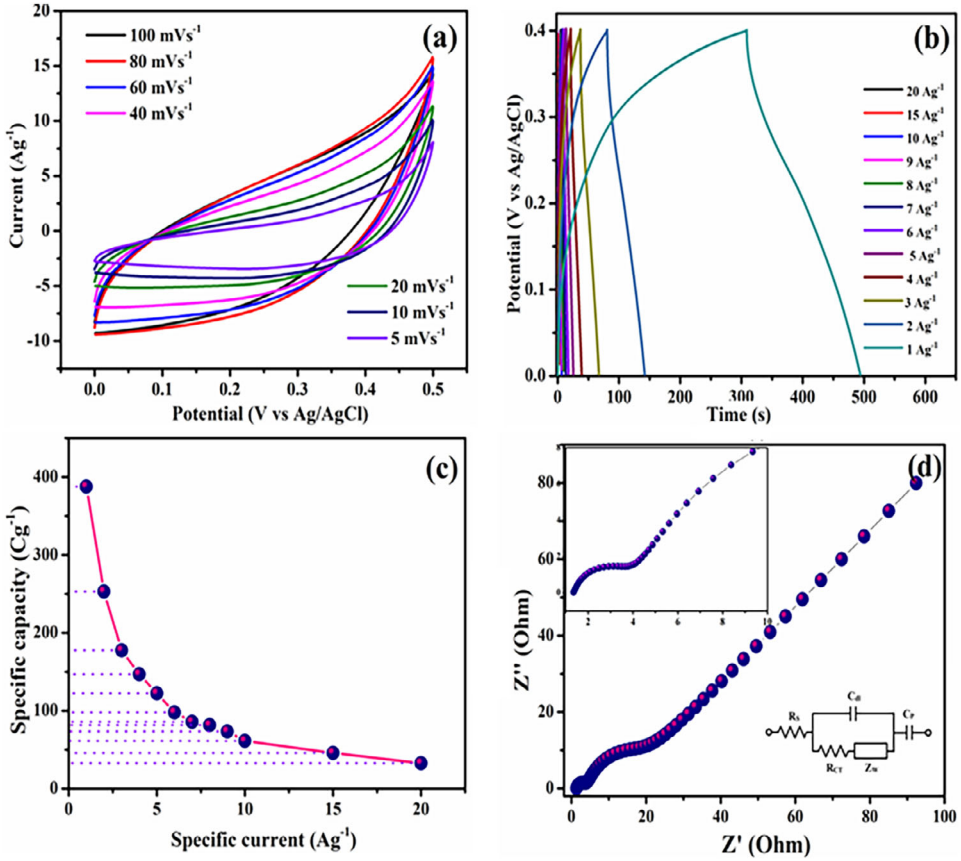

FIGURE 7 | Electrochemical characterization of CNZ nanocomposites: (a) Cyclic voltammograms at varying scan rates; (b) GCD profiles; (c) Current vs. potential at different current densities; (d) Nyquist plot with equivalent circuit model inset.

tion of nanostructures became advantageous for promoting fast chemical reactions within the boundary between electrodes and electrolytes.

Further, the observed results are compared well with the similar plant-synthesized mixed oxide electrodes and metal oxides electrodes prepared by some other methods. CuO-ZnO hybrid nanocomposites synthesized using *Ficus benghalensis* leaf extract can exhibit a specific capacitance of 352 Fg^{-1} at current density of 1 Ag^{-1} [74]. Green synthesis of CuO/NiO nanocomposite with different CuO/NiO ratios by *Saussurea costus* extract shows potent applications in energy storage technologies. The composite showed 1072 Fg^{-1} of capacitive performance along with 72% of capacitance retention even after 4000 cycles [75]. Krishnaiah et al. used neem extract to synthesize CuO–ZnO nanocomposite and studied their electrochemical performance, and the results revealed that the CuO–ZnO shows specific capacitance of 31 Fg^{-1} at the scan rate of 30 mVs^{-1} [76]. Flower-like nanocomposites based on ZnO/NiO as an effective electrode exhibit a specific capacity of 350 Cg^{-1} was found at 2 Ag^{-1} [77]. CuO-NiO nanocomposites synthesized via the hydrothermal method exhibit the specific capacitance of 35.63 Fg^{-1} at current density of 0.3 Ag^{-1} [78]. Ultrasound-assisted probe sonication route effectively prepared pure CuO and two-dimensional CuO-ZnO nanocomposites (NCs) for different ratios of CuO and ZnO, two-dimensional CuO-ZnO nanocomposites exhibited specific capacitance values that were found to be in the range of 248–352 Fg^{-1} [74]. The improvement in the specific capacitance of the composite electrode is the result of the nanoparticles are tightly bound to create composites with more surface area. The data shown in Figure 7c illustrates the change in specific capacitance values under various scan rates.

The composite electrode charge transport kinetics analysis occurred through the EIS spectra depicted in Figure 7d. The electrochemical impedance spectroscopy consists of two distinct regions: a semicircle in the high-frequency range and a straight line in the low-frequency range. The measurement data from the application of low-frequency range [79] appears as a semicircle that indicates resistance–capacitance parallel function, which other diffusion components lead to a high-frequency straight line [80]. The solution resistance (R_S) and charge transfer resistance (R_{CT}) reach values of 3.3 and 15.3 Ω, respectively, based on the X-intercept and diameter of the semi-circle. The low R_{CT} value detected in the electrode demonstrated that an intense reaction occurred between the electrode interface and electrolytic space because of efficient ionic conductivity. The ability to maintain electrode cycle performance stands as the essential criterion for utilizing materials in supercapacitor technology. The nanocomposite underwent a cycling stability test under 10 Ag^{-1} for 2000 cycles to evaluate its specific capacitance retention within KOH electrolytic solution. The researchers reported the cycle performance data after 2000 cycles of operation. The specific capacitance value of CNZ in KOH electrolyte remains almost 90% after measurement in Figure 8. The electrochemical parametric investigations demonstrated that this synthe-

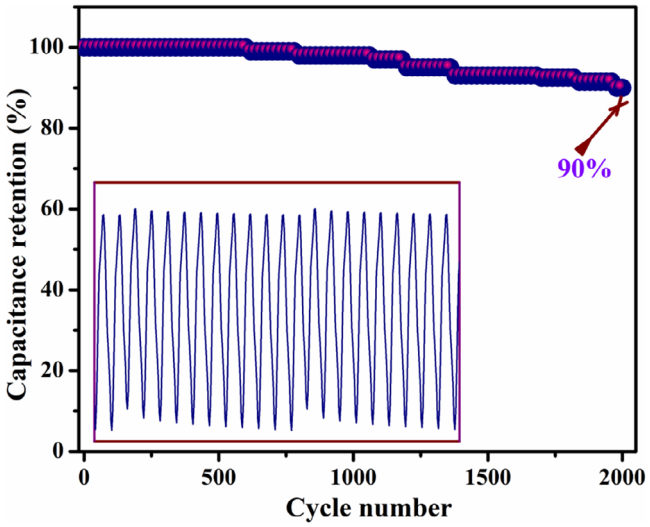

FIGURE 8 | Cyclic stability of the CNZ composite electrode.

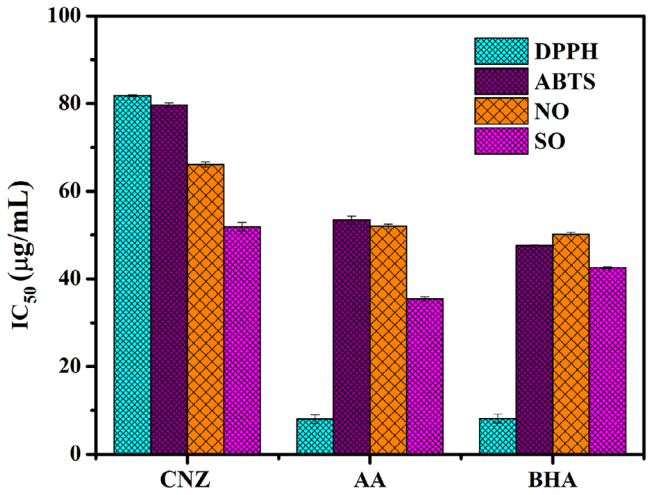

FIGURE 9 | Anti-oxidant activity of the **CNZ**.

sized material represents suitable materials for supercapacitor applications.

3.9 | Antioxidant Activity

Cell mutation caused by free radicals negatively affects human health. The elimination of ROS requires antioxidants as a necessary factor. In vitro antioxidant activity indicates their pharmacological function [81–84]. The investigation of $DPPH^{\bullet}$, $ABTS^{\bullet+}$, $NO^{\bullet}$, and O^{2-}, scavenging activity of synthesized nanocomposite (**CNZ**) appeared in Figure 9. Standards of pharmaceutical comparison consist of AA and BHA. Antioxidants within the test solution reduce the DPPH radical by donating electrons or hydrogen atoms, thus creating a change from violet to light yellow, along with a large reduction in maximum absorption. Researchers investigated the radical-scavenging percentage activity of the created nanocomposite across 20–100 μgmL^{-1} concentration levels. An increase in concentration leads to higher percentages of radical scavenging by the synthesized nanocomposite against the DPPH radical, as shown in Figure S3. The DPPH radical scavenging capability of **CNZ** possessed an IC_{50} value at 81.84 ± 0.15 μgmL^{-1} (Figure 9), but they showed significant activity compared to the standards such as AA (IC_{50} value at 7.98 ± 0.98 μgmL^{-1}) and BHA (IC_{50} value at 8.11 ± 1.02 μgmL^{-1}).

Free radical cations of $ABTS^{+}$ originate through nitrogen electron removal at the beginning of the experiment. ABTS undergoes oxidation when exposed to potassium persulfate or manganese dioxide and other similar agents, producing $ABTS^{+}$ free radicals. Antioxidants cause the $ABTS^{+}$ free radical to transform the solution into a colorless state [85]. Figure S4 demonstrates how CNZ lowers the activity of ABTS free radical scavenging throughout the entire test span. The anti-oxidant activity at 50 μgmL^{-1} concentration of CNZ reached 32% when tested with the ABTS compound, while normal ascorbic acid demonstrated 35%. The CNZ showed the most significant activity, with an IC_{50} of 79.70 ± 0.49 μgmL^{-1}, which was lower than that of the standards. The composite exhibits 78% inhibitory effect on nitric oxide at 100 μgmL^{-1} along with an IC_{50} value of 66.1 ± 0.65 μgmL^{-1} which was comparable one with the IC_{50} value of ascorbic acid (52.08 ± 0.56 μgmL^{-1}) according to the experimental results shown in Figure S5. At a concentration of 100 μgmL^{-1} the superoxide scavenging action of CNZ was measured at 85% which possessed 93% of the antioxidant capacity demonstrated by standard (AA, BHA) (Figure S6). The IC_{50} values of compounds CNZ, AA, and BHA were found to be 51.90 ± 0.95, 35.41 ± 0.56, and 42.60 ± 0.23 μgmL^{-1}, respectively. The anti-oxidant activity of the synthesized CNZ nanocomposite along with the control is given in Figure 9. From the results, we know that the CNZ possessed significant activity. Moreover, scavenging capability of CNZ was significantly comparable to that of standards (AA, BHA) at the same concentration ($p < 0.05$). It seemed that the scavenging ability of the synthesized composite exhibited good free radical scavenging activity, which are comparable to that of similar material synthesized via green methods [86–88].

4 | Conclusion

In conclusion, the research introduces an environment-friendly generation method by preparing copper, zinc, and nickel oxides based nanocomposites (CNZ) through *C. ternatea* flower extract. The synthesis procedure does not require chemical reagents because the flower extract bioactive compounds serve both as stabilizing and capping agents for generating nanoparticles. Multiple analytical techniques confirm the formation of the nanocomposite (CNZ) through this plant-assisted method. Electrochemical functionality based on CNZ electrode exhibited pseudocapacitive characteristics and achieved 387.7 Fg^{-1} specific capacitance at current density of 1 Ag^{-1}. The data show how CNZ nanocomposites can effectively function as energy storage components in supercapacitor devices. The antioxidant examination of CNZ nanocomposite included careful testing via four radical scavenging methods that utilized DPPH•, $ABTS^{\bullet+}$, NO• and O^{2-} assays. The CNZ nanocomposite shows antioxidant strength on equivalence with traditional antioxidants like ascorbic acid according to the test results. The promising features of CNZ make it a suitable candidate for pharmaceutical approaches and biomedical fields to reduce oxidative stress effects. This nanocomposite possesses special electrochemical properties combined with antioxidant functions that enable its utilization as energy

storage systems and antioxidant health agents. This investigation strengthens research on plant-based methods for nanomaterial production and introduces opportunities to study *C. ternatea* flower extract applications in nanotechnology and biomedical research.

Acknowledgments

The authors Kanagaraj Suganthi and Giriraj Kalaiarasi are grateful to Karpagam Academy of Higher Education Management for providing research support. Sheikdawood Parveen gratefully acknowledges DST for providing the Women Scientist Scheme—WOS (A) fellowship, Department of Science and Technology, New Delhi, India [Grant Number. SR/WOS(A)/CS-147/2021].

Conflicts of Interest

The authors declare no conflicts of interest.

Data Availability Statement

The data that support the findings of this study are available in the supplementary material of this article.

References

1. A. Faheem, M. M. Salem-Bekhit, F. Khan, S. Alshehri, A. Khan, M. M. Ghoneim, H. Wu, E. I. Taha, and E. Ibrahim, "Unique Properties of Surface-Functionalized Nanoparticles for Bio-Application: Functionalization Mechanisms and Importance in Application," *Nanomaterials* 12 (2022): 1333, https://doi.org/10.3390/nano12081333.

2. K. A. Altammar, "A Review on Nanoparticles: Characteristics, Synthesis, Applications, and Challenges," *Frontiers in Microbiology* 14 (2023): 1155622, https://doi.org/10.3389/fmicb.2023.1155622.

3. B. S. Hemanath, M. J. Deviprasad, and M. B. Shivaswamy, "Synthesis of Citral-Tryptamine Fused Selenium Nanospheres (CT@SeNP's) and Exploration of Their Anticancer, Antibacterial, and Electrochemical Sensor Applications," *Journal of Molecular Structure* 1310 (2024): 138240, https://doi.org/10.1016/j.molstruc.2024.138240.

4. K. Hachem, M. J. Ansari, and R. O. Saleh, "Methods of Chemical Synthesis in the Synthesis of Nanomaterial and Nanoparticles by the Chemical Deposition Method: A Review," *BioNanoScience* 12 (2022): 1032–1057, https://doi.org/10.1007/s12668-022-00996-w.

5. M. J. Deviprasad, B. S. Hemanath, and M. B. Shivaswamy, "Multifunctional Citral–Tryptamine Conjugated Silver Nanoparticles (CT@AgNPs): Antibacterial, Cytotoxicity, and Sensor Application," *BioNanoScience* 14 (2024): 5106–5121, https://doi.org/10.1007/s12668-024-01583-x.

6. S. Jeevitha, H. S. N. Prasad, and M. B. Shivaswamy, "Facile Green Preparation of $ZnFe_2O_4$ Nanoparticles Using Papaya Leaf Extract for Electrochemical Detection of Acetaminophen in Zerodol P and Dolo Drops," *Ionics* 30 (2024): 8617–8630, https://doi.org/10.1007/s11581-024-05879-6.

7. Z. Zhan, R. Dalan, and Z. Hu, "Reactive Oxygen Species Scavenging Nanomedicine for the Treatment of Ischemic Heart Disease," *Advanced Materials* 34 (2022): e2202169, https://doi.org/10.1002/adma.202202169.

8. R. Javed, M. Zia, S. Naz, S. O. Aisida, N. ul Ain, and Q. Ao, "Role of Capping Agents in the Application of Nanoparticles in Biomedicine and Environmental Remediation: Recent Trends and Future Prospects," *Journal of Nanobiotechnology* 18 (2020): 172, https://doi.org/10.1186/s12951-020-00704-4.

9. K. S. Y. Al Baloushi, A. Senthilkumar, K. Kandhan, R. Subramanian, J. Kizhakkayil, T. Ramachandran, S. Shehab, S. S. Kurup, M. A. M. Alyafei, A. S. Al Dhaheri, and A. Jaleel, "Green Synthesis and Characterization of Silver Nanoparticles Using Moringa Peregrina and Their Toxicity on MCF-7 and Caco-2 Human Cancer Cells," *International Journal of Nanomedicine* 19 (2024): 3891–3905, https://doi.org/10.2147/IJN.S451694.

10. S. Ali, A. Selva Sharma, W. Ahmad, M. Zareef, M. M. Hassan, A. Viswadevarayalu, T. Jiao, H. Li, and Q. Chen, "Noble Metals Based Bimetallic and Trimetallic Nanoparticles: Controlled Synthesis, Antimicrobial and Anticancer Applications," *Critical Reviews in Analytical Chemistry* 51 (2021): 454, https://doi.org/10.1080/10408347.2020.1743964.

11. A. Adaileh, A. H. Ragab, and M. A. Taher, "Development of Cu-ZnO ZrO_2 Based Polyacrylonitrile Polymer Composites for Removing Pharmaceutical Pollutants and Heavy Metals From Wastewater," *Scientific Reports* 15 (2025): 22250, https://doi.org/10.1038/s41598-025-95736-x.

12. C. Zhang, X. Wang, J. Du, Z. Gu, and Y. Zhao, "Reactive Oxygen Species-Regulating Strategies Based on Nanomaterials for Disease Treatment," *Advanced Science* 8 (2021): 2002797, https://doi.org/10.1002/advs.202002797.

13. H. F. Hetta, Y. N. Ramadan, and A. I. Al-Harbi, "Nanotechnology as a Promising Approach to Combat Multidrug Resistant Bacteria: A Comprehensive Review and Future Perspectives," *Biomedicines* 11 (2023): 413, https://doi.org/10.3390/biomedicines11020413.

14. K. Barathikannan, R. Chellaiah, V. Selvakumar, F. Elahi, M. Rubab, S. Sanyal, S. J. Yeon, and D. H. Oh, "Plant-Based Metabolites and Their Usesin Nanomaterials Synthesis: An Overview," *BioNanoScience* (2023): 1–22, https://doi.org/10.1007/978-981-99-0927-8_1.

15. N. Bisht, N. Dwivedi, and P. Kumar, "Recent Advances in Copper and Copper-Derived Materials for Antimicrobial Resistance and Infection Control," *Current Opinion in Biomedical Engineering* 24 (2022): 100408, https://doi.org/10.1016/j.cobme.2022.100408.

16. S. Udhaya Geetha and S. Thilakavathy, "Invitro DPPH Activity and Cytotoxicity Analysis of Zinc Oxide Nanoparticles (ZNONPS) From *Mangifera indica L. anacardiaceae* Leaves Extract," *International Journal of Health Sciences* 6 (2022): 5285–5293, https://doi.org/10.53730/ijhs.v6nS5.10137.

17. A. Serouti, L. S. Eddine, S. Meneceur, G. G. Hasan, H. A. Mohammed, C. Salmi, K. Iman, M. F. Ferhat, O. Ben Ali, and J. A. Ahmed Abdullah, "Biogenic ZnO/CuO/Fe_2O_3 Nanocomposite: A Groundbreaking Approach for Enhanced Degradation Capabilities and Reusability in Dye Removal Applications," *Arabian Journal for Science and Engineering* 49 (2024): 753–764, https://doi.org/10.1007/s13369-023-08495-0.

18. C. Li, W. Tang, and S. Chen, "Phytochemical Properties and in Vitro Biological Activities of Phenolic Compounds From Flower of *Clitoria ternatea L.*," *Molecules* 27 (2022): 6336, https://doi.org/10.3390/molecules27196336.

19. W. Widowati, L. Darsono, and M. R. Natariza, "Antidiabetic, Antidyslipidemia and Renoprotector Potency of Butterfly Pea Flower Extract (*Clitorea ternatea* L.) in Diabetes Mellitus and Dyslipidemia Rats Model," *Open Veterinary Journal* 14 (2024): 1135–1145, https://doi.org/10.5455/OVJ.2024.v14.i5.7.

20. A. Sharma, S. Ballal, D. Sharma, J. Pathak, A. A. AlGhamdi, S. Tadepalli, and I. Thangavelu, "Clitoria Ternatea Flower Extract Assisted Synthesis of Pluronic F127 and L-Histidine Coated SrO_2 as a Multimodality Nanocomposite for Anti-Cancer, Anti-Oxidant, and Antimicrobial Activities," *Bioprocess and Biosystems Engineering* 48 (2025): 1801–1816, https://doi.org/10.1007/s00449-025-03213-6.

21. T. Guttapalli, N. K. Rk, H. Rm, and K. Girigoswami, "rGO Decorated With ZnO Synthesized Using Clitoria Ternatea Flower Extract—Characterization, In Vitro and In Vivo Biocompatibility, and Textile Dye Remediation," *Journal of Composites Science* 9 (2025): 454, https://doi.org/10.3390/jcs9090454.

22. A. S. Kachhawaha, M. Elizabeth, P. Hari, A. Rajan, and N. Verma, "Green Synthesis and Antibacterial Evaluation of Iron Oxide Nanoparticles Using Clitoria Ternatea Flowers," *Biomedical and Pharmacology Journal* 18, no. 1 (2025): 749–759, https://doi.org/10.13005/bpj/3125.

23. S. Prabhu, T. D. Thangadurai, P. V. Bharathy, and P. Kalugasalam, "Synthesis and Characterization of Nickel Oxide Nanoparticles Using Clitoria Ternatea Flower Extract: Photocatalytic Dye Degradation Under Sunlight and Antibacterial Activity Applications," *Results in Chemistry* 4 (2022): 100285, https://doi.org/10.1016/j.rechem.2022.100285.

24. S. Prabhu, T. D. Thangadurai, and P. V. Bharathy, "Green-Based Biosynthesis of Zinc Oxide Nanoparticles Using Clitoria Ternatea Flower Extract and Its Antibacterial Activity," *Nano Biomedicine and Engineering* 13, no. 4 (2021): 394–400, https://doi.org/10.5101/nbe.v13i4.p394-400.

25. S. Prabhu, T. D. Thangadurai, P. V. Bharathy, and P. Kalugasalam, "Investigation on the Photocatalytic and Antibacterial Activities of Green Synthesized Cupric Oxide Nanoparticles Using *Clitoria ternatea*," *Iranian Journal of Catalysis* 12, no. 1 (2022): 1–11, https://doi.org/10.30495/ijc.2022.689547.

26. M. I. Alahmdi, S. Khasim, and S. Vanaraj, "Green Nanoarchitectonics of ZnO Nanoparticles From *Clitoria ternatea* Flower Extract for In Vitro Anticancer and Antibacterial Activity: Inhibits MCF-7 Cell Proliferation via Intrinsic Apoptotic Pathway," *Journal of Inorganic and Organometallic Polymers and Materials* 32 (2022): 2146–2159, https://doi.org/10.1007/s10904-022-02263-7.

27. Y. Y. Chan, Y. L. Pang, S. Lim, C. W. Lai, A. Z. Abdullah, and W. C. Chong, "Biosynthesized Fe- and Ag-Doped ZnO Nanoparticles Using Aqueous Extract of Clitoria Ternatea Linn for Enhancement of Sonocatalytic Degradation of Congo Red," *Environmental Science and Pollution Research* 27 (2020): 34675–34691, https://doi.org/10.1007/s11356-019-06583-z.

28. B. Satpathy, N. Sa, A. Behera, and P. K. Sahu, "Dose-Dependent Attenuation of the Efficacy of Clitoria Ternatea by Cobalt Oxide Nanoparticles Against Diabetes-Induced Cognitive Impairment," *Molecular Neurobiology* 62 (2025): 2601–2616, https://doi.org/10.1007/s12035-024-04436-6.

29. M. Lavanya and S. K. R. Namasivayam, "Eco-Friendly Fabrication of Magnesium Oxide Nanoparticles From *Clitoria ternatea* and Their Influence on Plant Growth Parameters of Vigna Mungo, Soil Nutrient Dynamics and Computational Analysis," *Plant Nano Biology* 14 (2025): 100200, https://doi.org/10.1016/j.plana.2025.100200.

30. S. Thulasi Krishnan, S. Parveen, A. S. El Newehy, G. Chandramohan, and G. Kalaiarasi, "Green Approaches for the Synthesis of Nickel Oxide and Cobalt Oxide Nanoparticles Towards Anti-Oxidant and Anti-Cancer Applications," *Journal of the Indian Chemical Society* 101 (2024): 101187, https://doi.org/10.1016/j.jics.2024.101187.

31. G. I. Edo, A. N. Mafe, A. B. M. Ali, P. O. Akpoghelie, E. Yousif, E. F. Isoje, U. A. Igbuku, S. A. Ismael, A. E. A. Essaghah, D. S. Ahmed, D. U. Ozsahin, H. Umar, and A. A. Alamiery, "Green Biosynthesis of Nanoparticles Using Plant Extracts: Mechanisms, Advances, Challenges, and Applications," *BioNanoScience* 15 (2025): 267, https://doi.org/10.1007/s12668-025-01883-w.

32. S. Zade, P. Pimpalshende, S. Toshniwa, and P. Chaware, "Pharmacognostical and phytochemical studies of Aparajita (Clitoria ternatea Linn.)," *International Journal of Pharmaceutical Sciences* 3 (2025): 3075–3097, https://doi.org/10.5281/zenodo.15282723.

33. R. R. Multisona, S. Shirodkar, M. Arnold, and A. G. Michalowska, "*Clitoria ternatea* Flower and Its Bioactive Compounds: Potential Use as Microencapsulated Ingredient for Functional Foods," *Applied Sciences* 13 (2023): 2134, https://doi.org/10.3390/app13042134.

34. G. C. Chavan, I. M. Jadhav, N. R. Jaiswal, S. S. Hardas, M. S. Kareppa, A. A. Kaware, and K. K. Zambare, "Traditional Herbaceous Plant *Clitoria ternatea*–A Review," *World Journal of Pharmacy and Pharmaceutical Sciences* 11 (2022): 1039–1047, https://doi.org/10.20959/wjpps20224-21753.

35. E. J. Jeyaraj, Y. Y. Lim, and W. S. Choo, "Antioxidant, Cytotoxic, and Antibacterial Activities of Clitoria Ternatea Flower Extracts and Anthocyanin-Rich Fraction," *Scientific Reports* 12 (2022): 14890, https://doi.org/10.1038/s41598-022-19146-z.

36. A. N. Abdulqodus, A. F. Abdulrahman, S. H. Mostafa, A. A. Kareem, S. M. Hamad, S. M. Ahmed, M. A. Almessiere, and D. Shaikhah, "Green Synthesis of ZnO Nanoparticles: Effect of pH on Morphology and Photocatalytic Degradation Efficiency," *Applied Physics A: Materials Science & Processing* 131 (2025): 720, https://doi.org/10.1007/s00339-025-08874-4.

37. M. Dehghani, B. Hajipour-Verdom, and P. Abdolmaleki, "Effect of Precipitating Agent, N_2 Gas, Extract Volume and pH on the Magnetic Properties of Magnetite Nanoparticles by Green Synthesis From Aqueous Pomegranate Peel Extract," *Front Chem* 12 (2024), https://doi.org/10.3389/fchem.2024.1413077.

38. M. Hemdan, E. Fayad, D. N. Binjawhar, F. G. Elsaid, and M. F. Mubarak, "Sustainable Graphene Oxide-ZIF-67-MOF/Avocado Pit-Derived Activated Carbon (GO-ZIF@APAC) Nanocomposite for Efficient Bisphenol a Adsorption From Aqueous Solutions: An Eco-Conscious Approach to Endocrine Disruptor Mitigation," *Surfaces and Interfaces* 72 (2025): 106920, https://doi.org/10.1016/j.surfin.2025.106920.

39. M. A. Farhat, A. Aridi, R. Yassine, Z. Bitar, and R. Awad, "Impact of Calcination Temperature on Structural and Optical Properties and Photocatalytic Efficiency of Ni0.33Cu0.33Zn0.33Fe2O4 Nanoparticles in Aniline Degradation," *Water, Air, & Soil Pollution* 235 (2024): 146, https://doi.org/10.1007/s11270-024-06932-w.

40. S. Athithyan, G. Kalaiarasi, and S. Parveen, "Facile Synthesis of Cobalt-Nickel Oxide Nanocomposites for Trifunctional Application Towards Antioxidant, Anticancer and Electrochemical Performance," *Inorganic Chemistry Communications* 164 (2024): 112384, https://doi.org/10.1016/j.inoche.2024.112384.

41. R. Re, N. Pellegrini, A. Proteggente, A. Pannala, M. Yang, and C. Rice-Evans, "Antioxidant Activity Applying an Improved ABTS Radical Cation Decolorization Assay," *Free Radical Biology and Medicine* 26 (1999): 1231–1237, https://doi.org/10.1016/S0891-5849(98)00315-3.

42. R. Ramalingam, A. R. Nath, B. B. Madhavi, M. Nagulu, and A. Balasubramaniam, "Free radical scavenging and antiepileptic activity of Leucas lanata," *Journal of Pharmacy Research* 6 (2013): 368–372, https://doi.org/10.1016/j.jopr.2013.03.011.

43. F. Wei, C. Jinglou, C. Yaling, L. Yongfang, C. Liming, and P. Lei, "Antioxidant, Free Radical Scavenging, Anti-Inflammatory and Hepatoprotective Potential of the Extract From *Parathelypteris nipponica* (Franch. et Sav.) Ching," *Journal of Ethnopharmacology* 130 (2010): 521–528, https://doi.org/10.1016/j.jep.2010.05.039.

44. B. M. Olabinri, O. O. Odedire, M. T. Olaleye, A. S. Adekunle, L. O. Ehigie, and P. F. Olabinri, "In Vitro Evaluation of Hydroxyl and Nitric Oxide Radical Scavenging Activities of Artemether," *Research Journal of Biological Sciences* 5 (2010): 102, https://doi.org/10.3923/rjbsci.2010.102.105.

45. N. Y. Elamin, M. R. Elamin, and B. Y. Abdulkhair, "Eco-Friendly Alginate–Sulfonated Bagasse Biochar/Zeolitic Imidazolate Framework-8 Nanocomposite for Efficient Mercury(II) Removal: Synthesis, Mechanism, and Regeneration Performance," *Colloids and Surfaces A: Physicochemical and Engineering Aspects* 725 (2025): 137557, https://doi.org/10.1016/j.colsurfa.2025.137557.

46. E. Gobinath, M. Dhatchinamoorthy, P. Saran, D. Vishnu, R. Indumamathy, and G. Kalaiarasi, "Synthesis and Characterization of NiO Nanoparticles Using Sesbania Grandiflora Flower to Evaluate Cytotoxicity," *Results in Chemistry* 6 (2023): 101043, https://doi.org/10.1016/j.rechem.2023.101043.

47. Z. Sabri Abbas, M. M. Kadhim, and A. Rheima, "Preparing Hybrid Nanocomposites on the Basis of Resole/Graphene/Carbon Fibers for Investigating Mechanical and Thermal Properties," *BioNanoScience* 13 (2023): 983–1011, https://doi.org/10.1007/s12668-023-01119-9.

48. T. Munawar, F. Iqbal, S. Yasmeen, K. Mahmood, and A. Hussain, "Multi Metal Oxide NiO-CdO-ZnO Nanocomposite–Synthesis, Structural, Optical, Electrical Properties and Enhanced Sunlight Driven

Photocatalytic Activity," *Ceramics International* 46 (2020): 2421–2437, https://doi.org/10.1016/j.ceramint.2019.09.236.

49. Y. B. Chan, V. Selvanathan, L.-H. Tey, M. Akhtaruzzaman, F. H. Anur, S. Djearamane, A. Watanabe, and M. Aminuzzaman, "Effect of Calcination Temperature on Structural, Morphological and Optical Properties of Copper Oxide Nanostructures Derived From *Garcinia Mangostana* L. Leaf Extract," *Nanomaterials* 12 (2022): 3589, https://doi.org/10.3390/nano12203589.

50. E. Fayad, D. N. Binjawhar, F. G. Elsaid, A. Taha, and M. F. Mubarak, "Innovative CuZnCr-BTC Framework for Enhanced Congo Red Dye Removal in Sustainable Wastewater Treatment," *Journal of Cluster Science* 36 (2025): 125, https://doi.org/10.1007/s10876-025-02840-z.

51. N. A. S. K. Anuar and C. K. Sheng, "Structural and Morphological Characterization of CuO Nanostructure Precipitated by Water-Soluble Copper (II) Nitrate Hemi(Pentahydrate) and NaOH as Reactants," *Journal of Nano- and Electronic Physics* 13 (2021): 05015, https://doi.org/10.21272/jnep.13(5).05015.

52. S. M. Botsa, R. Dharmasoth, and K. Basavaiah, "A Facile Synthesis of Cu2O and CuO Nanoparticles via Sonochemical Assisted Method," *Current Nanoscience* 15 (2018): 209–213, https://doi.org/10.2174/1573413714666180530085447.

53. S. D. Dhas, P. S. Maldar, and M. D. Patil, "Synthesis of NiO Nanoparticles for Supercapacitor Application as an Efficient Electrode Material," *Vacuum* 181 (2020): 109646, https://doi.org/10.1016/j.vacuum.2020.109646.

54. A. K. Atul, S. K. Srivastava, A. K. Gupta, and N. Srivastava, "Synthesis and Characterization of NiO Nanoparticles by Chemical Co-Precipitation Method: An Easy and Cost-Effective Approach," *Brazilian Journal of Physics* 52 (2022): 2, https://doi.org/10.1007/s13538-021-01006-2.

55. S. Wirunchit and W. Koetniyom, "ZnO Nanoparticles Synthesis and Characterization by Hydrothermal Process for Biological Applications," *Physica Status Solidi A Applications and Material Science* 329 (2025): 147904, https://doi.org/10.1002/pssa.202200364.

56. M. Patel, S. Mishra, R. Verma, and D. Shikha, "Synthesis of ZnO and CuO Nanoparticles via Sol Gel Method and Its Characterization by Using Various Technique," *Discover Materials* 2 (2022): 1, https://doi.org/10.1007/s43939-022-00022-6.

57. K. Karthik, S. Dhanuskodi, C. Gobinath, S. Prabukumar, and S. Sivaramakrishnan, "Ultrasonic-assisted CdO–MgO nanocomposite for multifunctional applications," *Materials Technology* 34 (2019): 403, https://doi.org/10.1080/10667857.2019.1574963.

58. M. Z. Ishaque, Y. Zaman, A. Arif, A. B. Siddique, M. Shahzad, D. Ali, M. Aslam, H. Zaman, and M. Faizan, "Fabrication of Ternary Metal Oxide (ZnO: NiO: CuO) Nanocomposite Heterojunctions for Enhanced Photocatalytic and Antibacterial Applications," *RSC Advances* 13 (2023): 30838–30854, https://doi.org/10.1039/D3RA05170F.

59. A. O. Juma, E. A. A. Arbab, C. M. Muiva, L. M. Lepodise, and G. T. Mola, "Synthesis and Characterization of CuO-NiO-ZnO Mixed Metal Oxide Nanocomposite," *Journal of Alloys and Compounds* 723 (2017): 866–872, https://doi.org/10.1016/j.jallcom.2017.06.288.

60. N. A. Bhatt, L. Quigley, and S. Zhou, "Morphology and Property Tuning in ZnO–Ni Hybrid Metamaterials in Vertically Aligned Nanocomposite (VAN) Form," *Nanoscale Advances* 7 (2025): 3528–3538, https://doi.org/10.1039/D5NA00207A.

61. A. Modwi, M. A. Ghanem, A. M. Al-Mayouf, and A. Houas, "Lowering Energy Band Gap and Enhancing Photocatalytic Properties of Cu/ZnO Composite Decorated by Transition Metals," *Journal of Molecular Structure* 1173 (2018): 1–6, https://doi.org/10.1016/j.molstruc.2018.06.082.

62. G. A. Alharshan, A. Almohammedi, M. A. M. Uosif, E. R. Shaaban, and M. Emam-Ismail, "Impact of Heat Treatment on the Structural, Optical, Magnetic and Photocatalytic Properties of Nickel Oxide Nanoparticles," *Materials* 16 (2024): 4146, https://doi.org/10.3390/ma17164146.

63. S. Pallavi, P. Choudhary, A. Yadav, B. Dewangan, V. N. Rai, and A. Mishra, "Improved Structural and Dielectric Properties of Cd and Ti Dual Doped ZnO Nanoparticles," *Applied Physics A* 126 (2020): 1, https://doi.org/10.1007/s00339-020-03943-2.

64. A. Dastider, H. Saha, M. J. F. Anik, M. Jamal, and M. M. Billah, "Second Phase Cu 2 O Boosted Photocatalytic Activity of Fluorine Doped CuO Nanoparticles," *RSC Advances* 14 (2024): 11677–11693, https://doi.org/10.1039/D3RA08790E.

65. D. Paul, S. Mangla, and S. Neogi, "Antibacterial Study of CuO-NiO-ZnO Trimetallic Oxide Nanoparticle," *Materials Letters* 271 (2020): 127740, https://doi.org/10.1016/j.matlet.2020.127740.

66. J. S. Mohammed, M. A. Hasan, H. J. Alatta, M. I. Abd-AL Majied, K. Ali Jasim, A. H. Shaban, and R. Abd Al-Zahra Fadil, "Investigate the Structural Properties of Tl1-xHgxSr2Ca2Cu3O8+δ Compound by Using Scherrer Modified Equation," *AIP Conference Proceedings* 2769 (2023): 020064, https://doi.org/10.1063/5.0129140.

67. K. R. Desai, S. T. Alone, and S. R. Wadgane, "x-Ray Diffraction Based Williamson–Hall Analysis and Rietveld Refinement for Strain Mechanism in Mg–Mn Co-Substituted $CdFe_2O_4$ Nanoparticles," *Physica B: Condensed Matter* 614 (2021): 413054, https://doi.org/10.1016/j.physb.2021.413054.

68. S. Parveen, S. Balakrishnan, A. Shanmugapriya, J. J. William, G. Kalaiarasi, and H.-H. Nguyen, "Cobalt Schiff Base Complex as Battery-Type Electrode for Supercapacitor Applications," *Inorganic Chemistry Communications* 178 (2025): 114572, https://doi.org/10.1016/j.inoche.2025.114572.

69. S. Pal Singh, A. Kumari Singh, and P. Yadav, "Synthesis and Characterization of Structural and Optical Properties of Ni-Doped Zinc Sulfide Nanoparticles," *Journal of Advanced Scientific Research* 13 (2022): 87, https://doi.org/10.55218/JASR.202213416.

70. E. Kacan, "Optimum BET Surface Areas for Activated Carbon Produced From Textile Sewage Sludges and Its Application as Dye Removal," *Journal of Environmental Management* 166 (2016): 116–123, https://doi.org/10.1016/j.jenvman.2015.09.044.

71. Y. Z. Zhang, Y. Wang, and Y. L. Xie, "Porous Hollow Co_3O_4 With Rhombic Dodecahedral Structures for High-Performance Supercapacitors," *Nanoscale* 6 (2014): 14354–14359, https://doi.org/10.1039/C4NR04782F.

72. K. Kannan, K. Chinnaiah, K. Gurushankar, et al., "Investigation of the Electrochemical Behavior of CuO-NiO-Co_3O_4 Nanocomposites for Enhanced Supercapacitor Applications," *Materials* 17 (2024): 3976, https://doi.org/10.3390/ma17163976.

73. W. Fan, Q. Wang, and K. Rong, "MXene Enhanced 3D Needled Waste Denim Felt for High-Performance Flexible Supercapacitors," *Nano-Micro Letters* 16 (2023): 36, https://doi.org/10.1007/s40820-023-01226-y.

74. A. BaQais, M. W. Alam, M. Farhan, G. Muteeb, N. Allag, and S. Mushtaq, "Probe-Sonicated Synthesis of CuO–ZnO Hybrid Nanocomposite for Photocatalytic and Supercapacitor Applications," *Inorganics* 11 (2023): 370, https://doi.org/10.3390/inorganics11090370.

75. E. Da'na, N. Parveen, A. Taha, and M. R. El-Aassar, "CuO/NiO Nanocomposite Prepared With *Saussurea costus* Extract for Super-Capacitor Energy Storage Application," *Nanocomposites* 10 (2024): 283, https://doi.org/10.1080/20550324.2024.2363733.

76. C. V. Krishnaiah and D. K. Behara, "Photocatalytic and Electrochemical Sensor Studies of CuO-ZnO Nanocomposite Synthesized via Green Combustion Using Neem Leaf Extract," *Materials Science and Technology* (2025), https://doi.org/10.1177/02670836251367107.

77. N. S. Alsaiari, M. Ahmad, and I. Shaheen, "Three-dimensional Flower-Like Nanocomposites Based on ZnO/NiO as Effective Electrode Materials for Supercapacitors," *Journal of Electroanalytical Chemistry* 930 (2023): 117158, https://doi.org/10.1016/j.jelechem.2023.117158.

78. S. Chatterjee, A. Ray, M. Mandal, and S. K. Bhattacharya, "Synthesis and Characterization of CuO-NiO Nanocomposites for Electrochemical

Supercapacitors," *Journal of Materials Engineering and Performance* 29 (2020): 8036–8048, https://doi.org/10.1007/s11665-020-05261-3.

79. H. Ju, Q. Tang, and Y. Xu, "Prussian Blue Analogue-Derived Hollow Metal Oxide Heterostructure for High-Performance Supercapacitors," *Dalton Transactions* 52 (2023): 12948–12957, https://doi.org/10.1039/D3DT01966G.

80. S. Balasundari, S. Jayasubramaniyan, and P. Thangavel, "Heterostructure CuO/Co_3O_4 Nanocomposite: An Efficient Electrode for Supercapacitor and Electrocatalyst for Oxygen Evolution Reaction Applications," *ACS Applied Engineering Materials* 1, no. 1 (2023): 606–615, https://doi.org/10.1021/acsaenm.2c00146.

81. S. Pinchujit, A. Phuruangrat, and S. Wannapop, "Synthesis and Characterization of Heterostructure Pt/Bi2WO6 Nanocomposites With Enhanced Photodegradation Efficiency Induced by Visible Radiation," *Solid State Sciences* 134 (2022): 107064, https://doi.org/10.1016/j.solidstatesciences.2022.107064.

82. O. Yayapao, T. Thongtem, A. Phuruangrat, and S. Thongtem, "Synthesis and Characterization of Highly Efficient Gd Doped ZnO Photocatalyst Irradiated With Ultraviolet and Visible Radiations," *Materials Science in Semiconductor Processing* 39 (2015): 786–792, https://doi.org/10.1016/j.mssp.2015.06.039.

83. Y. Liu, X. Li, and X. Li, "Highly Permeable WO3/CuWO4 Heterostructure With 3D Hierarchical Porous Structure for High-Sensitive Room-Temperature Visible-Light Driven Gas Sensor," *Sensors and Actuators B: Chemical* 365 (2022): 131926, https://doi.org/10.1016/j.snb.2022.131926.

84. Y. Liu, T. Wong, and X. Huang, "Skin-Integrated, Stretchable, Transparent Triboelectric Nanogenerators Based on Ion-Conducting Hydrogel for Energy Harvesting and Tactile Sensing," *Nano Energy* 99 (2022): 107442, https://doi.org/10.1016/j.nanoen.2022.107442.

85. P. Basnet, T. Inakhunbi Chanu, D. Samanta, and S. Chatterjee, "A Review on Bio-Synthesized Zinc Oxide Nanoparticles Using Plant Extracts as Reductants and Stabilizing Agents," *Journal of Photochemistry and Photobiology B: Biology* 183 (2018): 201–221, https://doi.org/10.1016/j.jphotobiol.2018.04.036.

86. T. J. Masho, P. T. Arasu, R. F. Bogale, E. A. Zerrefa, and S. Ramamurthy, "Green Synthesis, Characterization of $Ag_2O/CuO/ZnO$ Nano Composites Using Aqueous Extract of Croton Macrostachyus Leaf for Photo Degradation, Anti-Microbial and Antioxidant Activities," *Results in Chemistry* 7 (2024): 101369, https://doi.org/10.1016/j.rechem.2024.101369.

87. J. Khan, S. Bibi, and I. Naseem, "Ternary Metal (Cu–Ni–Zn) Oxide Nanocomposite via an Environmentally Friendly Route," *ACS Omega* 8, no. 23 (2023): 21032–21041, https://doi.org/10.1021/acsomega.3c01896.

88. S. R. Bavaji and A. J. Ahamed, "Synthesis of Cu Doped NiO for Their Antioxidant and Photocatalytic Properties: Green Synthesis Using *Lycopodium linn*," *Chemical Physics Impact* 8 (2024): 100647, https://doi.org/10.1016/j.chphi.2024.100647.

Supporting Information

Additional supporting information can be found online in the Supporting Information section.

UV–Vis spectroscopic data of the nanocomposite (CNZ), Williamson-Hall (W-H) plot and anti-oxidant assays graphs have been given in the Supporting Information.

Supporting file: slct71943-sup-0001-SuppMat.docx